An electrochemical evaluation on the crevice corrosion of 430 stainless steel by micro capillary tubing method

EUN-YOUNG NA
Research Institute of Energy Resources Technology, Chosun University, Gwangju, 501-759, Korea
E-mail: eyna@chosun.ac.kr

Published online: 12 April 2006

The aim of this study was to investigate the initiation of crevice corrosion for ferritic 430 stainless steel in artificial crevice electrode cells using the IR drop mechanism. The 430 stainless steel artificial crevice electrodes were potentiodynamically polarized in solutions of sodium chloride with different concentrations. The potentiostatic polarization was measured for various artificial crevice sizes by measuring the potentials in the crevice by the depth profile technique using a micro capillary tube which was inserted into the crevice. The criterion for IR$>\Delta\ \Phi^*$, where $\Delta\ \Phi^*$ is the difference between the applied potential, E_{SURF}, and the electrode potential of the active/passive transition, $E_{A/P}$, was also measured during the process of crevice corrosion. The potentials in the crevice were successfully measured from −220 mV versus SCE to −360 mV versus SCE, which is lower than that of the external surface potential of −200 mV versus SCE. Thus these results show that evaluation of corrosion using the IR drop mechanism in the crevice was more objective and easier to reproduce than the existing methods.

1. Introduction

Ferritic stainless steel is an Fe-Cr series alloy containing 12–30% Cr which retains its body centered cubic structure even after heat treatment in the normal temperature range [1]. Its corrosion resistance and strength improve with increasing Cr content. Furthermore, it is an inexpensive material, since no Ni is used. Austenite stainless steel is very sensitive to stress corrosion cracking in a hot chloride environment, whereas, ferritic stainless steel is known to be extremely resistant to such an environment. [2–4]. Therefore, the use of ferritic stainless steel in automobiles, domestic electric appliances, and water heaters is on the increase. Meanwhile, the phenomenon of crevice corrosion is very difficult to examine in detail, due to the variation in the time and location of corrosion initiation and velocity of corrosion propagation [5], which causes the results obtained with the crevice corrosion study method to be difficult to reproduce, thereby making it difficult to explain the mechanism of progression of crevice corrosion. In addition, despite the increasing consumption of ferritic stainless steel, little research has been done on crevice corrosion. The existing mechanisms of crevice corrosion rely solely on acidification, mass transport, and other features, but completely exclude the electrode potential, E, and its distribution, E_x, within the crevice cell. The IR drop mechanism focuses on the outer surface of the passive sample and the difference in electric potential that exists inside the crevice. That is, active crevice corrosion can develop at a certain inside the crevice while the outer surface of the sample still maintains the passive state. Especially, it has been proven by several researchers that there is an IR drop inside the crevice, which has been shown experimentally and by mathematical modeling to be related to the IR drop theory, and is thought to be involved in the progression of crevice corrosion originating from chemical changes in the crevice solution. [6–11]. However, studies involving the electrochemical evaluation of crevice corrosion are limited by the small size of the crevices. Also, in previous studies, the IR mechanism during the crevice corrosion induction period was not able to be identified.

Therefore, this study focuses on ferritic 430 stainless steel, which shows great potential in various fields of application, but for which problems of reproducibility have been encountered in previous studies involving the crevice corrosion method. The size of the artificial crevice was 0.1 mm, 0.2 mm and 0.5 mm sample. The solution, which is an important factor in the corrosion environment, was

0022-2461
DOI: 10.1007/s10853-005-5679-0

TABLE I Composition of 430 stainless steel

Elements	Weight percent
Fe	82.26
Cr	16.46
Ni	0.32
Mn	0.50
Si	0.36
Mo	0.0024
P	0.035
S	0.004
C	0.055

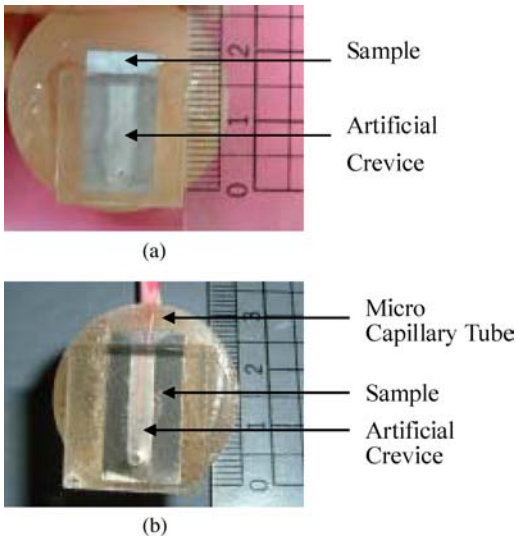

Figure 1 Experimental sample used for crevice corrosion test; (a) crevice corrosion sample, and (b) assembly of micro capillary tube & sample.

also made separately, and the experiment was conducted based on the potentiostatic polarization, by measuring the current density-time curve in each solution. Additionally, the potential drop inside the crevice was measured by inserting a micro capillary tube into it; in order to examine the mechanism of crevice corrosion related to the IR drop.

2. Experimental procedures

The typical composition of 430 stainless steel is shown in Table 1. All of the samples used in this study measured $10\times20\times5$ mm and were obtained from the as received sheet material. They were mounted in a fast curing epoxy with a copper wire soldered on one side, and ground to expose the 10×20 mm crevice surface. The 430 stainless steels were mechanically ground with increasingly fine SiC paper through 1200 grits and finally polished with aluminum oxide (Al_2O_3) powder. Prior to the study, the samples were cleaned ultrasonically with ethyl alcohol. The 3×16 mm artificial crevice was formed in the same position on each sample and three different crevice widths were used, viz. 0.1, 0.2 and 0.5 mm, and the crevices were formed using Plexiglas. The experimental sample containing the artificial crevice and the micro capillary tube placed in the crevice are shown in Fig. 1. The electrode potential on the crevice wall could be measured by positioning the micro capillary tube at the vertical boundary on the crevice wall. Fig. 2 shows the experimental apparatus. A potentiostat CMS-100 electrochemical corrosion measuring system manufactured by Gamry Corp was used for this experiment equipment. A carbon rod and a saturated calomel electrode (SCE) were used for the counter and reference electrodes respectively. All potentials are referenced to the SCE.

All test solutions were prepared in the laboratory. 1N H_2SO_4 solution was used as the corrosion solution for the passivation of the surface, and NaCl solution made using double distilled water and used at room temperature acted as the source of Cl^- ions, which are known to break down the passive film. Four concentrations of NaCl, viz. 0.01N, 0.05N, 0.1N and 0.5N, were selected to control for the effect of Cl^- ion concentration. For the electrochemical evaluation method, we utilized the potentiodynamic polarization test with a scanning speed of 600 mV/hr from -600 mV versus SCE to -1200 mV versus SCE in the positive direction, and analyzed the corrosion behavior, including the corrosion potential and passive current density. Then, the potentiostatic polarization test was used to measure the passive current density and crevice corrosion initiation time. N_2 gas was passed through the apparatus

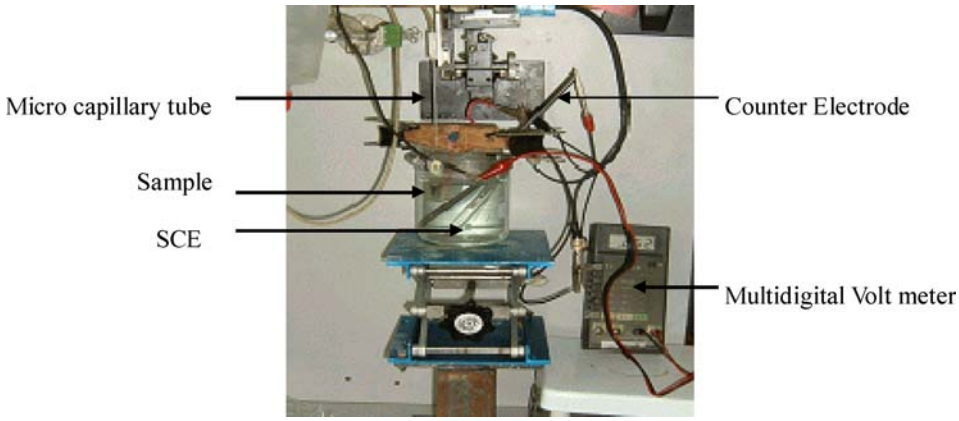

Figure 2 Experimental apparatus.

at a flow rate of 150 cm^3/min for 30 minutes before the test in order to ensure that the experiment was conducted under clean conditions.

3. Results and discussion

The anodic polarization curve of 430 stainless steel in the four sulfuric acid solutions containing different concentrations of sodium chloride (1N H_2SO_4 + 0.01N, 0.05N, 0.1N and 0.5N NaCl) shows a large active peak consisting of a low-current passive region for the scan performed in the passive-to-active direction. These results are shown in Fig. 3 and Table II. These curves indicate that the corrosion electric potential values tended to decrease when the sodium chloride concentration was increased. On the other hand, the critical current density values and the passive current density increased as the pitting potential value decreased. However, these data show that the passive region attained -200 mV versus SCE for each of the sodium chloride concentrations. The influence of the sodium chloride concentration on the crevice corrosion initiation time can also be observed in the potentiostatic polarization curves.

Fig. 4 shows the current density-time curve, which presents the dependence of the current density value on the elapsed time. The current density inside the crevice increased, while the crevice corrosion initiation time (i.e. the time at which the passive film starts to break down inside crevice) decreased, as the sodium chloride concentration was increased. On the other hand, at a low concentration such as 0.01 N, the sodium chloride did not show any crevice corrosion during the entire testing period of 86,400 seconds (24 h). However, for the sodium chloride concentrations of 0.05 N, 0.1 N and 0.5 N the crevice corrosion initiation times were 1720 seconds (29 minutes), 1,408 seconds (23 minutes) and 550 seconds (9 minutes), respectively. The corresponding current densities were 0.96, 1.87, and 6.60 mA/cm^2, respectively.

Next, we confirmed the constant potential of −200 mV versus SCE, which is the passive section potential of the corrosion solution, 1 N H_2SO_4 + 0.1 N NaCl. The potentiostatic polarization test was performed using a fixed artificial crevice size of 3 × 16 mm (depth × length) and various widths, viz. 0.1 mm, 0.2 mm and 0.5 mm, in order to measure the dependence of the current change inside the crevice on the elapsed time. The crevice size-dependent potentiostatic polarization test results are shown in Fig. 5. It was observed that the crevice corrosion developing time for widths of 0.1 mm and 0.2 mm were 905 seconds (15 minutes) and 1,408 seconds (23 minutes), respectively. However, in the case where the width was 0.5 mm, no sudden change of current was observed during the entire test period of 32,000 seconds (9 hours). From these observations, it was confirmed that the crevice corrosion initiating critical crevice size is between 0.2 and 0.5 mm. Also, the maximum current densities inside the crevice for widths 0.1 mm and 0.2 mm were 5.50 and 1.87 mA/cm^2, respectively, whereas for a width of 0.5 mm the passive current density value did not change.

This effect is similar to that observed both outside and inside of the crevice when ion-cells such as those resulting when a Cl^- ion concentration difference or dissolved oxygen concentration difference is formed [12, 13]. It was also shown that when the width of the crevice is large, the

TABLE II Anodic polarization data for 430 stainless steel for different sodium chloride concentrations

NaCl concentration	Corrosion potential (mV/SCE)	Critical current density (mA/cm^2)	Passivation current density (mA/cm^2)	Break down potential (mV/SCE)
0.01 N	−517	6.31	0.03	951
0.05 N	−523	15.85	0.05	949
0.1 N	−539	25.12	0.06	921
0.5 N	−554	31.62	0.63	142

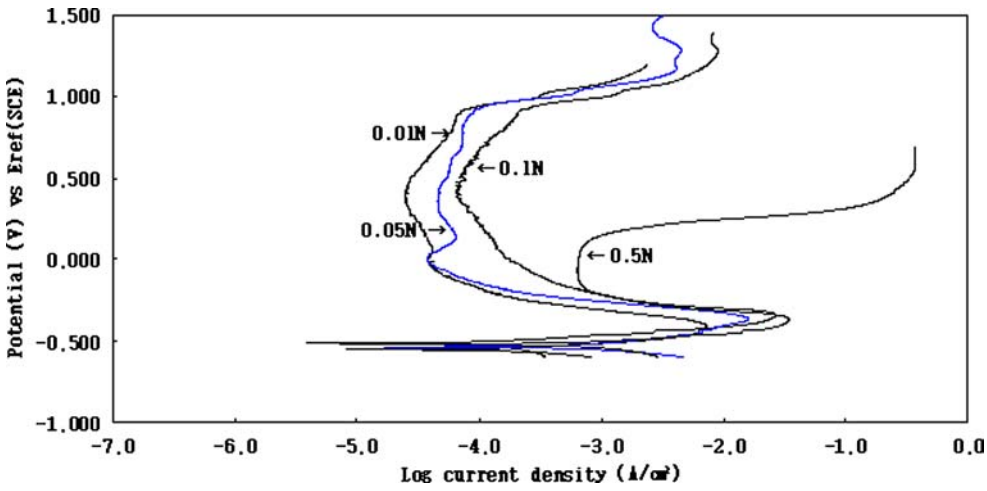

Figure 3 Polarization curves of 430 stainless steel in different concentrations of sodium chloride.

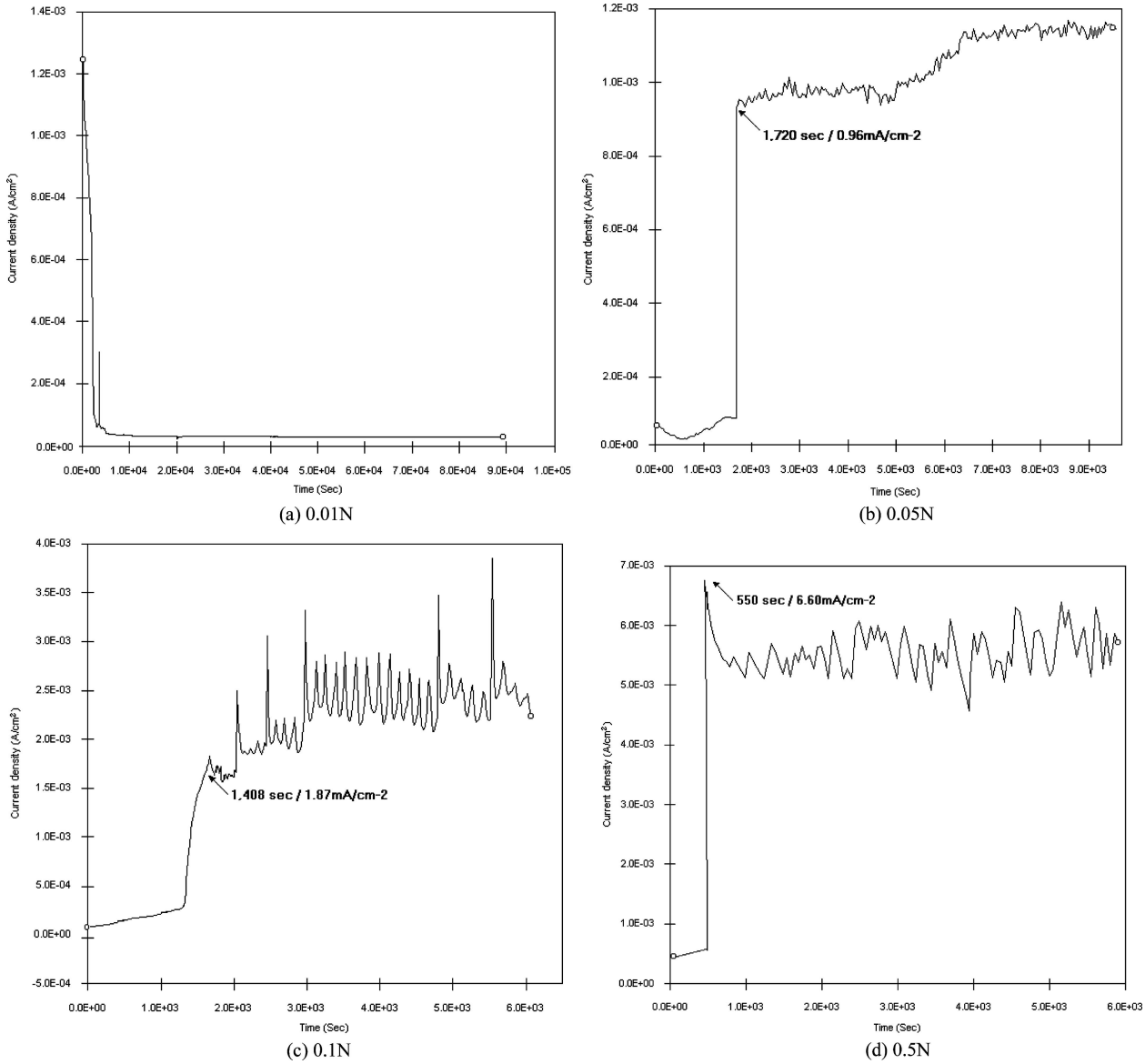

(a) 0.01N (b) 0.05N

(c) 0.1N (d) 0.5N

Figure 4 The relation between the current density and time for crevice corrosion in 1 N sulfuric acid solution with different sodium chloride concentrations; (a) 0.01N, (b) 0.05N, (c) 0.1N, and (d) 0.5N.

solution ions or oxygen transfer well through the outside and inside of the crevice, causing the concentration difference to decreases, with the result that crevice corrosion does not occur. Potentiostatic experiments were also conducted with samples placed in the upside-down orientation, and in which a potential of −200 mV versus SCE in the passive region of the polarization curve was applied to the crevice samples with different solutions and crevice widths. The results are shown in Fig. 6. Even though a passive potential of −200 mV versus SCE is applied to the crevice, because the crevice depth is more than 1 mm, due to the resulting potential drop, the passive potential reaches −220 mV versus SCE. This kind of crevice corrosion is brought into the active region by the IR drop, thus causing the corrosion to increase. It was shown in this experiment that the transfer of the corrosion potential values into the active region of the potentiodynamic polarization curves is the main cause of crevice corrosion.

There are numerous studies in the literature in which the switch of IR $< \Delta\ \Phi*$ to IR$> \Delta\ \Phi^*$ could have ended the induction period and initiated the onset of crevice corrosion at the bottom of the crevice. Some authors recognized this possibility to some extent. A recent example is the study of stainless steel in dilute NaCl solution by Brossia and Kelly [14] although these authors did not go any further than to note that a solution-composition-change and crevice width change were operative during the induction period. Also, many past localized corrosion studies need to be reexamined in a new light since, in some cases, the authors concluded without the benefit of the recent advances made in this area of research, that the IR mechanism was not operating in their study. The IR drop inside the crevice is thought to result from the following

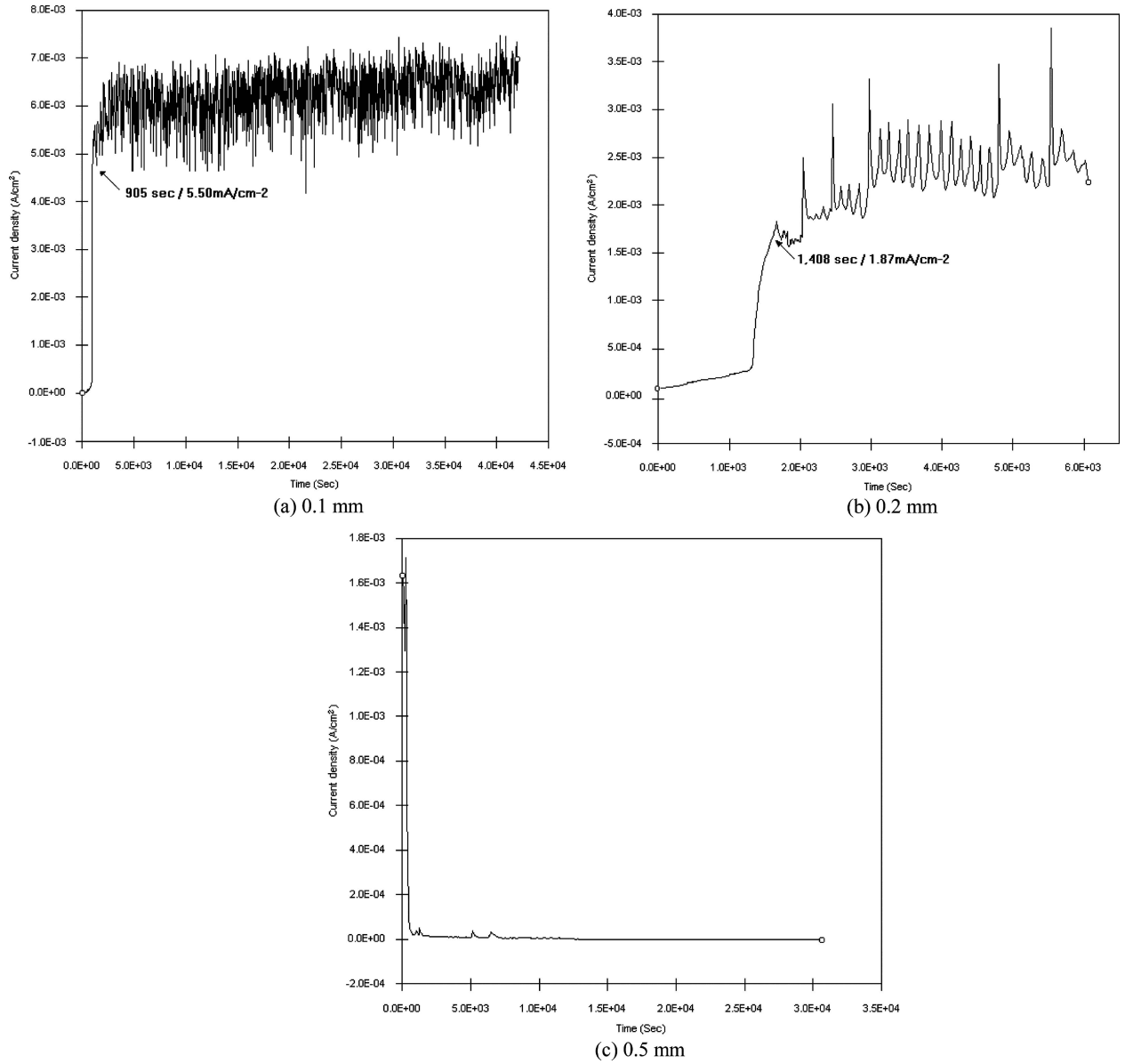

Figure 5 The relation between the current density and time for the crevice corrosion of 430 stainless steel in 1 N H_2SO_4 + 0.1 N NaCl at 20°C with a crevice size of 3 × 16 mm and various widths; (a) 0.1 mm, (b) 0.2 mm, and (c) 0.5 mm.

mechanism; certain aggressive ions (notably Cl^- and H^+) are promoted to transfer inside the solution and this results in a change in the local chemical reaction inside the crevice, causing the breakdown of the passive film. As a result the potential inside the crevice becomes lower than that on the outside, due to the different rates of ion transfer inside and outside of the crevice. Meanwhile, according to the study conducted by Pickering and Frankenthal, among the different passive breakdown mechanisms caused by a drop in the IR the ions (Fe^{2+}, $FeOH^+$, H^+, OH^-, Na^+, Cl^-, etc.) inside the crevice are controlled by diffusion, electrical transfer and chemical reaction [15]. A potential difference appears at the opening and the bottom of the crevice, thus breaking down the passive film and, since crevice corrosion causes the IR drop to be increased, this mechanism is proposed in the form of a theoretical, mathematical modeling [16]. Also, Pickering reported that if the potential of ferrous alloys drops more than the critical potential difference ($IR > \Phi^*$), the current density will rapidly increase and, consequently, metal with crevices will develop more corrosion [17].

However, in this study we used a new method, namely the micro capillary tube, to investigate the high potential difference which is observed between the bottom and opening of the crevice, and which is quite difficult to explain with the theory of crevice corrosion initiation based on the chemical changes of the crevice solution. Moreover the main factor in the initiation of crevice corrosion is thought to be the geometrical aspects of the crevice, such as the width and depth. Fig. 7 shows the crevice corrosion states of 430 stainless steel for different crevice sizes. Crevices with sizes of 0.1 mm and 0.2 mm tended

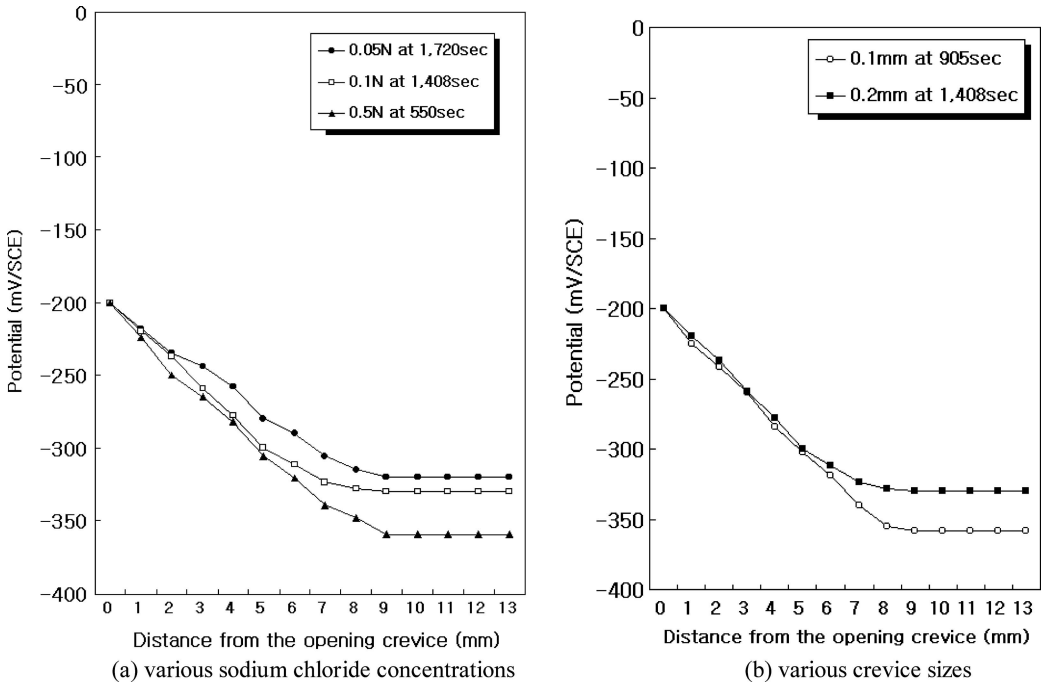

(a) various sodium chloride concentrations (b) various crevice sizes

Figure 6 Measured electrode potential profiles inside a crevice in the upside-down orientation.; (a) various sodium chloride concentrations and (b) various crevice sizes.

(a) (b) (c)

Figure 7 Photographs of crevice corrosion samples in 1 N H_2SO_4 + 0.1 N NaCl with different crevice widths; (a) 0.1 mm, (b) 0.2 mm, and (c) 0.5 mm.

to have more severe corrosion in the opening than at the bottom, whereas crevices with a size 0.5 mm did not develop any corrosion. Fig. 8 shows a picture of a sample with a size of 0.1 mm. Fig. 8 (a) shows the front side of the half-cut sample, (b) shows the side view of the corrosion part with cubic effects, and (c) shows the side view of the corrosion part for the purpose of depth measurement. Therefore, the maximum depth of the crevice on the corrosion sample was found to be 1 mm, as measured from the surface of the crevice.

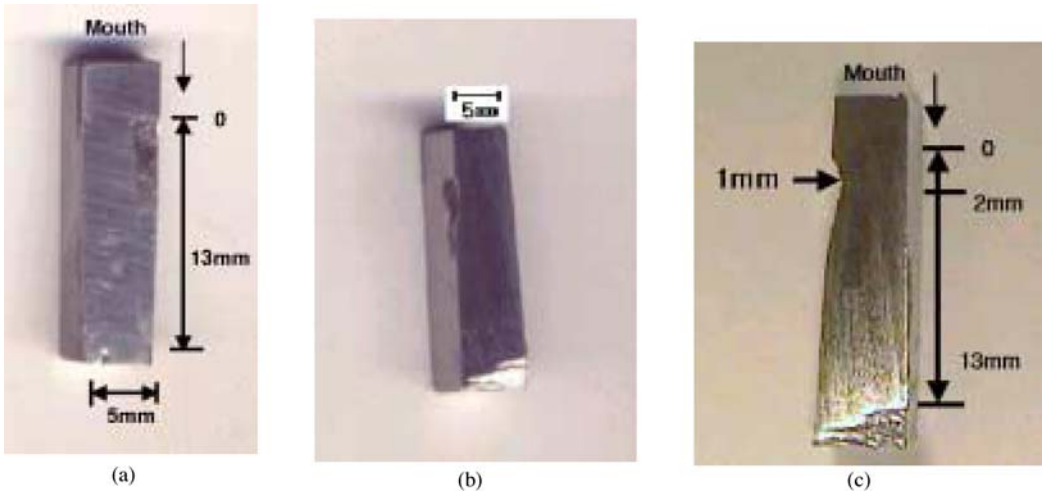

(a) (b) (c)

Figure 8 Photographs of the surface of 430 stainless steel in 1 N H_2SO_4 + 0.1N NaCl with a crevice size of 3×0.1×16 mm; (a) Front, (b) Lateral geometry, and (c) Lateral.

4. Conclusion

The crevice corrosion of ferritic stainless steel was investigated by the micro capillary tube method from the electrochemical point of view by measuring the potentiostatic polarization.

1. The E_{cor} (corrosion potential) and E_b (pitting potential) decreased as the NaCl concentration increased. On the other hand, the i_{crit} (critical current concentration) values and i_p (passive current density) increased as the NaCl concentration increased. Also, the crevice corrosion rapidly increased as the NaCl concentration increased, but no crevice corrosion occurred at a concentration of 0.01N during the entire testing period.

2. The crevice corrosion initiation time shortened and the current density values increased as the width of the crevice decreased, but no crevice corrosion was observed when the width of the crevice was 0.5 mm. We were able to confirm that the critical crevice size for initiating crevice corrosion is between 0.2 and 0.5 mm. The potentiostatic polarization test results showed that the turning point of the depth-location potential inside the crevice matched that of the time-dependent current density inside the crevice.

3. Even though the presence of a passive state potential of −200 mV versus SCE potential was confirmed on the sample surface, the passive film was broken down. By measuring the potential change due to crevice depth from the outside of the crevice, it was determined that the current density increased and the corrosion rapidly increased when the critical potential difference exceeded 20 mV, thereby causing the interior of the crevice to be placed in the active state. Therefore, we were able to confirm that the crevice corrosion of ferritic 430 stainless steel increases when the corrosion part of the interior of the crevice is put in the active state. Thus, these results show that the evaluation of corrosion based on the IR drop mechanism in the crevice was more objective and easier to reproduce than the existing methods.

References

1. W. F. SMITH, in "Principles of Materials Science and Engineering" (McGraw-Hill, New York, 1990) 55.
2. D. A. JONES, in "The Principles and Prevention of Corrosion" (Macimillan publishing Co., 1992) 198.
3. W. C. LESILE, in "The Physical Metallurgy of Steels" (McGraw-Hill, New York, 1981) 326.
4. K. R. TRECHEWEY and J. CHAMBERLAIN, in "Corrosion for Science and Engineering", 2nd edn. (Longman Scientific and Technical, 1995) 165.
5. M. S. DESA and C. M. RANGEL, *Br. Corrosion Jr.*, **23** (1988) 186.
6. K. CHO and H. W. PICKERING, *J. Electrochem. Soc.* **137** (1990) 3313.
7. Y. XU and H. W. PICKERING, *ibid.* **140** (1993) 658.
8. B. A. KEHLER, G. O. ILEVBARE and J. R. SCULLY, *Corrosion Jr.* **57** (2001) 1042.
9. K. CHO, M. I. ABDULSALAM and H. W. PICKERING, *J. Electrochem. Soc.* **145** (1998) 1862.
10. M. WANG and H. W. PICKERING, *J. Electrochem. Soc.* **142** (1995) 2986.
11. B. A. SHAW, P. J. MORAN and P. O. GARTLAND, *Corros. Sci.* **32** (1991) 707.
12. A. J. BETTS and L. H. BOULTON, *Br. Corrosion Jr.* **28** (1993) 279.
13. S. P. TRASATTI and F. MAZZA, *ibid.* **31** (1996) 105.
14. C. S. BROSSIA and R. G. KELLY, *Corros. Sci.* **40** (1998) 1851.
15. H. W. PICKERING and R. P. FRANKENTHAL, *J. Electrochem. Soc.* **119** (1972) 1297.
16. A. VALDES and H. W. PICKERING, "Advances in Localized Corrosion" edited by H. Isaacs, U. Bertocci, J. Kruger, and S. Smialowska, Huston, TX, (1990) 393.
17. Y. XU, M. WANG and H. W. PICKERING, *J. Electrochem. Soc.* **140** (1993) 1448.

Received 3 March
and accepted 25 July 2005